



INSTITUT DE FRANCE
Académie des sciences

Comptes Rendus

Physique

Thomas Pardoen, Nathan Klavzer, Sarah Gayot, Frederik Van Loock, Jérémy Chevalier, Xavier Morelle, Vincent Destoop, Frédéric Lani, Pedro Camanho, Laurence Brassart, Bernard Nysten and Christian Bailly

Nanomechanics serving polymer-based composite research


Volume 22, issue S3 (2021), p. 331-352

<<https://doi.org/10.5802/crphys.56>>

Part of the Special Issue: Plasticity and Solid State Physics

Guest editors: Samuel Forest (Mines ParisTech, Université PSL, CNRS, France) and David Rodney (Université Claude Bernard Lyon 1, France)

© Académie des sciences, Paris and the authors, 2021.
Some rights reserved.

 This article is licensed under the
CREATIVE COMMONS ATTRIBUTION 4.0 INTERNATIONAL LICENSE.
<http://creativecommons.org/licenses/by/4.0/>



*Les Comptes Rendus. Physique sont membres du
Centre Mersenne pour l'édition scientifique ouverte*
www.centre-mersenne.org



Nanomechanics serving polymer-based composite research

Thomas Pardoen^{*,a}, Nathan Klavzer^a, Sarah Gayot^{a,b}, Frederik Van Loock^a,
Jérémy Chevalier^c, Xavier Morelle^d, Vincent Destoop^a, Frédéric Lani^c,
Pedro Camanho^e, Laurence Brassart^f, Bernard Nysten^b and Christian Bailly^b

^a Institute of Mechanics, Materials and Civil engineering (iMMC), UCLouvain, B-1348 Louvain-la-Neuve, Belgium

^b Institute of Condensed Matter and Nanosciences - Bio and Soft Matter (IMCN/BSMA), UCLouvain, B-1348 Louvain-la-Neuve, Belgium

^c Solvay, Material Science Application Center (MSAC), B-1120 Bruxelles, Belgium

^d Laboratoire d'Ingénierie des Matériaux Polymères, CNRS UMR n°5223, INSA de Lyon, 69100 Villeurbanne, France

^e Departamento de Engenharia Mecânica, Faculdade de Engenharia, Universidade do Porto, Rua Dr. Roberto Frias 4200-465 Porto, Portugal

^f Department of Engineering Science, University of Oxford, OX1 3PJ Oxford, United Kingdom

E-mails: thomas.pardoen@uclouvain.be (T. Pardoen), nathan.klavzer@uclouvain.be (N. Klavzer), sarah.gayot@uclouvain.be (S. Gayot), frederik.vanloock@uclouvain.be (F. Van Loock), jeremy.chevalier@solvay.com (J. Chevalier), morelle.xavier@gmail.com (X. Morelle), vincent.destoop@uclouvain.be (V. Destoop), frederic.lani@solvay.com (F. Lani), pcamanho@fe.up.pt (P. Camanho), laurence.brassart@eng.ox.ac.uk (L. Brassart), bernard.nysten@uclouvain.be (B. Nysten), christian.bailly@uclouvain.be (Ch. Bailly)

Abstract. Tremendous progress in nanomechanical testing and modelling has been made during the last two decades. This progress emerged from different areas of materials science dealing with the mechanical behaviour of thin films and coatings, polymer blends, nanomaterials or microstructure constituents as well as from the rapidly growing field of MEMS. Nanomechanical test methods include, among others, nanoindentation, in-situ testing in a scanning or transmission electron microscope coupled with digital image correlation, atomic force microscopy with new advanced dynamic modes, micropillar compression or splitting, on-chip testing, or notched microbeam bending. These methods, when combined, reveal the elastic, plastic, creep, and fracture properties at the micro- and even the nanoscale. Modelling techniques including atomistic simulations and several coarse graining methods have been enriched to a level that allows treating complex size, interface or surface effects in a realistic way. Interestingly, the transfer of this paradigm to advanced long fibre-reinforced polymer composites has not been as intense compared to other fields. Here, we show that these methods put together can offer new perspectives for an improved characterisation of the response at the elementary fibre-matrix level, involving the interfaces and interphases. Yet, there are still many open issues left to resolve. In addition, this is the length scale, typically below 10 micrometres,

* Corresponding author.

at which the current multiscale modelling paradigm still requires enhancements to increase its predictive potential, in particular with respect to non-linear plasticity and fracture phenomena.

Keywords. Nanomechanics, Nanoindentation, DIC, Polymer-based Composites, AFM.

Funding. The authors are thankful to Audrey Favache for her support in the use of nanoindentation. NK is mandated by the Belgian National Fund for Scientific Research (FSR-FNRS), XM was mandated by FSR-FNRS and JC was mandated by FNRS-FRIA. SG, TP and CB acknowledge the support of ARKEMA. Part of the research has been funded by the Belgian National Fund for Scientific Research (FSR-FNRS) under Grant T.0178.19 and part by the Walloon Region under the agreements RW7281 – TECCOMA and RW 47911 – VISCOS in the context of the SKYWIN Pole of competitiveness.

Available online 4th March 2021

1. Introduction

The field of mechanics of polymer-based composites has dramatically evolved since the turn of the millennium. This evolution was doped and structured by the multiscale approach of the mechanical behaviour of materials. Multiscale modelling is indeed today the preferred paradigm to link materials characteristics to their end-use properties, and to combine into a single vision the materials science quest to develop better materials and the structural mechanics objective to accurately predict the integrity of composite components. The core of the multiscale approach relies on the development of micromechanics-based models, scale transition formalisms, and the necessary accompanying numerical methods that allow integrating the fibre-matrix elementary level up to the full composite level [1–5]. The computational modelling methods have been supplemented by rich new experimental data emerging from 3D in situ tomography [6–8] and 2D or 3D digital image/volume correlation methods (DIC/ DVC), see e.g. [9–13]. These experiments provide an invaluable source of information to build physical scenarios for the deformation and failure history and to validate the models, supplementing classical macro-mechanical tests. Recently, multiscale modelling approaches have been aided by machine learning methods to accelerate the simulations and/or the optimisation analysis [14–16].

Nevertheless, many fundamental questions remain regarding the material response at the lower length scale, which is the one of the fibre-matrix elementary volume – i.e. typically below 10 micrometres. Outstanding questions include:

- (1) (a) Is the local mechanical behaviour of the matrix similar to the behaviour measured on bulk thermoset or thermoplastic samples? Contradictory data have been reported and will be discussed in the paper. When a difference is found between bulk and “in-between fibres” behaviour, the next two questions ensue:
 - (b) Is the matrix material located in micrometre-sized volumes in between closely spaced fibres intrinsically different in terms of, for instance, molecular mass, cross-linking density, anisotropy, degree of crystallinity in thermoplastics or free volume as a result of the specific local curing conditions?
 - (c) Or is the difference in behaviour the result of a mechanical confinement effect that modifies the development of plasticity, similar to a strain gradient plasticity effect in metals, see e.g. [17], also known to play a role in polymers [18]?
- (2) Are the fracture mechanisms in the matrix comparable to those occurring in bulk samples and if not, what are the fundamental failure mechanisms within the matrix? In bulk specimens, fracture is often dominated by the nucleation of microcracks on micrometre-sized defects [19] that are not observed in confined matrix regions. Recent reports show that an epoxy resin specimen of small dimensions can be very ductile compared to a larger bulk specimen [20–23].

- (3) What is the mechanical response of the interface and interphase region between the fibre and matrix? An interphase layer, modified by the presence of fibre sizing and by the associated change of polymerization conditions, is known to develop near the fibre surface. The literature indicates such region thickness to range from a few nanometres to micrometres. The load transfer to the fibre, the possible plastic localisation and the resistance to decohesion will be considerably affected by the elastic and plastic characteristics of this interlayer with respect to the surrounding matrix.
- (4) What is the link between the nature of the interphase layer and the possibility of a preferential path for diffusion and/or for ageing leading to evolving mechanical strength and damage resistance?
- (5) What is the internal stress field existing at the scale of the confined matrix after curing, if any, and how does it relax with time?
- (6) The longitudinal tensile failure of composites is, to a large extent, determined by the Weibull fibre strength distribution and by the stress redistribution resulting from the failure of individual fibres. Some outstanding open questions include a possible “in-situ” Weibull fibre strength distribution that differs from that measured in the tests conducted in dry fibres/tows, and the magnitude of stress concentration gradients across undamaged fibres located close to a broken one [24,25].

Convincing quantitative answers to these questions could significantly enhance both the predictive capabilities of multiscale models and the capacity to pro-actively guide composite design towards novel principles for tougher materials.

The natural approach available today is to address the previous questions by borrowing from nanomechanical methods developed mainly for other material classes and, for some of them, from the solid state physics community, and apply them at the scale of interest, as schematically shown in Figure 1. Nanomechanical methods involve on the experimental side: nanoindentation mapping, quantitative atomic force microscopy (AFM) mapping, push-in or push-out tests, in-situ testing in a scanning electron microscope (SEM) combined to DIC, in-situ testing by x-ray microtomography coupled to DVC, micropillar compression from focused ion beam (FIB) machining; and on the modelling side: molecular dynamics (MD) studies, mesoscale shear transformation zone (STZ)-based models (developed in the context of transition state theory, borrowed from solid state physics) and advanced viscoelastic viscoplastic models with or without length scale dependencies. Some of these methods also provide information about the chemistry and structure of the polymer matrix.

The objective of this paper is to describe how some of these nanomechanical approaches can be and have been applied at the fibre-matrix elementary level, and how they can be combined to develop a more quantitative understanding of the local mechanical behaviour. The paper will not provide definitive responses to the questions raised above – and that will certainly remain on the roadmap for many years to come –, but will deliver some guidelines on possible answers. The presentation will illustrate the messages with results from our own studies, involving some already published data as well as some new results¹, while obviously recognising that more and more groups worldwide are working on this subject. A vast majority of these examples will focus on a standard composite material system comprising an epoxy matrix (RTM6) and carbon fibres (CF), which is a material system widely used in aeronautical applications.

¹ The new results concern the size effect observed in nanoindentation, the analysis of the constraint effect associated to the fibres affecting the extraction of the modulus from nanoindentation data, and the fibre push out tests obtained on this system.

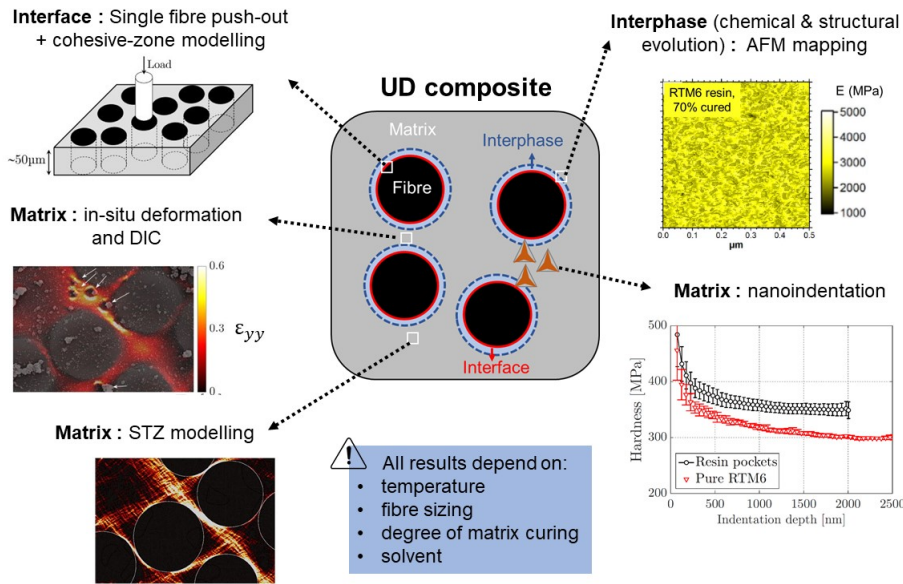


Figure 1. Description of some nanomechanics-based methods to quantitatively investigate the response of the matrix-fibre elementary volume, involving the confined matrix, the interphase layer, the interface with fibre and the fibre.

2. Nanoindentation

Nanoindentation allows the non-destructive measurement of several mechanical properties such as hardness and elastic indentation modulus at the micro- and nanoscales, and the extraction of constitutive model characteristics through inverse modelling [26, 27]. In a nanoindentation test, a sharp pyramidal (or conical) tip with a radius of curvature typically below 100 nm penetrates into the material under load, followed by an unloading sequence, see Figure 2a. Classical nanoindentation can be defined as a depth-sensing indentation (DSI) method. The continuous stiffness measurement (CSM) mode, which superimposes an oscillatory displacement on the main loading, is used to continuously measure hardness and elastic modulus and can be used to perform nano-DMA tests. This is necessary in polymers, for which indentation size effects similar to metals are usually observed [26, 28, 29]. The common theoretical approach to extract stiffness and hardness from the load-displacement curve is based on the Oliver and Pharr method [30] following the work of Sneddon [31]. This method gives the contact area based on the actual indentation depth h_c evaluated using the sink-in correction of the material around the indenter, see Figure 2a. In case of pile-up, the model by Loubet et al. is considered to be more appropriate [32].

The use of nanoindentation for the characterisation of pure polymer specimens remains a topic of controversy in the literature [33, 34] as the elastic modulus extracted with this method is often higher than the one determined with macroscale tests on the same polymer samples [34–36]. The difference is sometimes attributed to Oliver and Pharr's theoretical approach, which relies on elastic contact mechanics to describe a viscoelastic material. Additionally, the effects of pile-up under the indenter due to plasticity, viscoelasticity, hydrostatic stress and fibre constraint strongly affect the measured properties by, for instance, over- or underestimating the contact area. Hence, these factors cast doubt on the inherent accuracy of the material property measurement via nanoindentation [37]. Several models and correction factors have been proposed to address this issue: these allowed some authors to get corrected modulus values lying

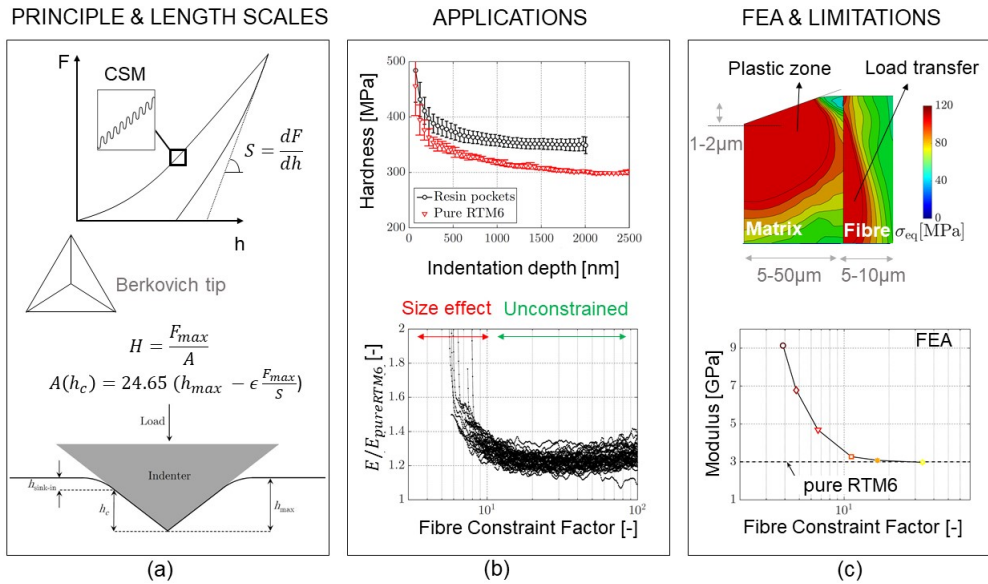


Figure 2. Application of nanoindentation to extract stiffness and hardness of polymer matrix in near-fibre confined volumes; (a) principle of nanoindentation; (b) example of hardness and elastic stiffness data in highly cross-linked RTM6 epoxy measured by nanoindentation, comparing bulk and confined values - the fibre constraint factor is the distance to fibre normalized by indentation depth; (c) finite element simulation of nanoindentation to account for and deconvolute the fibre constraint effect.

within $\pm 5\%$ of the values obtained via macro-scale tests [36,38]. Size effects also affect the indentation response: a decrease of hardness and modulus values is detected in the first few hundreds of nanometres below the surface, until a plateau is reached at a threshold depth. This size effect can be attributed to both length scale dependent elasticity and/or plasticity effects, and to interactions with the intrinsic dimensions of the polymer structure such as the radius of gyration of the molecules [39–42]. Hence, despite these unresolved challenges, nanoindentation measurements have been used to feed FE simulations [38,43,44], showing the potential of combining this approach with more advanced matrix continuum constitutive models.

The determination of the in-situ properties of polymer matrices within fibre-reinforced polymer composites (FRPs) adds another level of complexity to the nanoindentation data extraction. As indicated in the introduction, the presence of fibres in FRPs affects the curing process of the matrix, potentially modifying its mechanical properties within matrix pockets. A difference in property measured by nanoindentation on pure polymers vs. FRPs using the exact same product has been repetitively reported, the latter exhibiting higher hardness and modulus even when the aforementioned correction factors are accounted for [45,46]. Finite element studies demonstrated that a sub-surface stress transfer mechanism between the matrix and the fibres is present, giving rise to an extrinsic fibre constraint effect, which must be deconvoluted to determine any true changes of the material properties [47,48], see Figure 2c. Hence, it is important to consider matrix pocket size, fibre proximity and indentation depth when measuring the in-situ properties of a composite matrix. Recently, Chevalier [49] studied the mechanical response of an epoxy matrix (RTM6) within carbon fibre unidirectional (UD) composites. The indentation results on pure RTM6 were in good agreement with other earlier studies [28,39,50], see Figure 2b. The bulk indentation results were compared with the ones in resin-rich composite pockets, with the lat-

ter providing 20% higher hardness and elastic modulus values. By looking at the effect of the distance to the closest fibre, the hardness was found relatively insensitive to the fibre constraint. FEA results related this observation to a decrease in the sink-in amplitude close to the fibres. Conversely, the modulus proved to be significantly impacted by fibre proximity. Finite element analyses based on an advanced classical continuum elasto-viscoplastic model [51] reproduced with fidelity both effects, see Figure 2c. However, the FEA does not quantitatively capture the higher absolute hardness values measured in the composite specimens with respect to those obtained in the pure polymer, even in large matrix pockets where the plastic zone below the indenter is not influenced by the closest fibres, see Figure 2c. Furthermore, it is obvious that the FEA – which is based on a model with no internal length – scale does not capture the size effect at lower indentation depth, except if considering an unrealistically blunt indenter tip. The size effect at low indentation depths thus most presumably results from the constrained mobility of the polymer chains under the indenter, calling for more advanced constitutive model developments.

Ultimately, these studies highlight the limits of classical nanoindentation protocols to deal with polymeric materials. Nonetheless, progress in instrumentation and the use of FEA allow the determination of valuable microscale properties that can be used to either elucidate the underlying deformation or feed multiscale FE models. Finally, note that the minimum penetration depth required to provide reliable results in classical DSI is rarely much below 100 nm. This leads to probed volumes with characteristic dimensions close to or just below one micrometre, making it inappropriate to determine gradients of properties in the expected interphase region between fibre and matrix and giving one reasons, among several others, to look for Atomic force microscopy (AFM)-based methods.

3. Atomic force microscopy

Atomic force microscopy [52] is used for the surface analysis of materials at the nanometre scale. AFM probes consist of a flexible micro-cantilever terminated by a microscopic tip with a nanometric apex that interacts with the surface. As the scanning probe encounters modifications of the surface topography and/or different materials, the tip-surface interaction forces vary, causing variations of the vertical deflection of the cantilever (contact mode) or modifying the oscillation parameters of the cantilever (tapping™ mode). Topographic imaging of the sample as well as mapping of some physical properties (e.g. elastic modulus) can be derived from these variations of the cantilever deflection or of its oscillatory behaviour. Note that hybrid DSI-AFM systems also exist, where the indenter tip also serves as a scanning probe: it is dragged over the surface before and after indentation in order to obtain topographic images. The main advantage of this technique is the possibility to locate flat regions well-suited for indentation. However, the topographic image of the indented surface is often of poor quality, due to the indenter damaging the sample surface during scanning [33]. In the same idea, interfacial force microscopy (IFM) was developed in the early 1990's [53]. The tip radius is similar to that used in the hybrid DSI-AFM systems, but smaller forces may be applied during indentation leading to less surface damage and better spatial resolution [33]. AFM has been used since the 1990's in the field of composite materials for the micro- and nanoscale analysis of matrix properties [54, 55] and the mechanical characterisation of interphases [56–69]. As shown in Figure 3, subtle property variations can occur over nanometric distances in such systems (e.g. degree of matrix curing [54]), which asks for excellent spatial resolution involving both measurement sensitivity and accuracy. With a nominal tip radius generally close to or smaller than 10 nm, AFM can provide nanoscale spatial resolution [69], see Figure 3. Yet, until the late 2000's, mechanical mapping with AFM mostly led to qualitative results. Phase imaging in tapping™ mode could yield “relative stiffness maps” with excellent contrast, but the phase signal could hardly be related to any intrinsic material

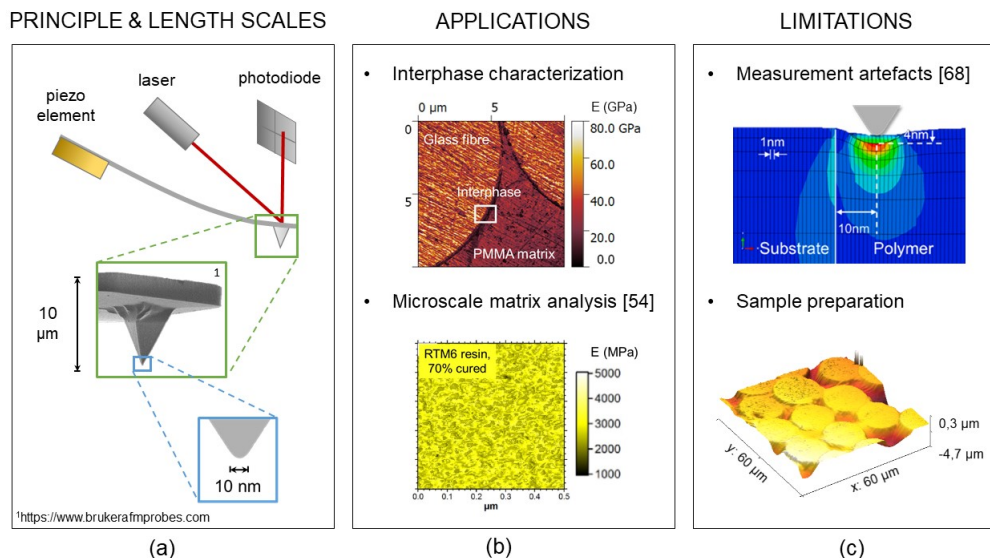


Figure 3. Characterisation of polymer-based composites by AFM: (a) instrumentation and length scales, (b) applications and (c) current limitations.

property [58, 70] as it depends on the energy dissipation during the tip-sample contact (which itself may be due to several properties of the material). Force-modulation AFM (FM-AFM) [71] and force-volume imaging [72] were the first methods developed in the 1990's [33, 56–58] for performing mechanical mapping with AFM. However, generating images in force-volume mode was very time-consuming [70, 73] and imaging in force-modulation mode led to erroneous modulus values due to the tip and surface damage induced by the contact mode and to the variation of the contact area when the tip scanned regions of different rigidity [58].

Since then, many other modes have been developed with the objective of being able to quantitatively map mechanical properties in a reasonable amount of time. All these modes are based on a vertical modulation of the probe position, either at one of its resonance frequencies or off-resonance. For example, the PeakForce tapping mode (PFT, off-resonance mode) [73] and the HarmoniX™ mode (resonance mode) [74] both allow, after proper calibration, a quantitative mapping of various mechanical properties (modulus, adhesion, indentation, etc.) simultaneously with a 3D topographic imaging of the surface [67, 69, 75]. Smaller indentation forces (in the pN to nN range, see e.g. [67, 69, 70, 73]) are used compared to nanoindentation techniques (μN range [56, 58]), which also improves spatial resolution and measurement sensitivity and accuracy. Two examples of nanoscale quantitative mapping performed on composite-related samples are illustrated in Figure 3:

- (1) an assessment of modulus homogeneity in a partially-cured RTM6 epoxy matrix [54] and,
- (2) a mechanical characterisation of the interphase region in a fibre-reinforced methacrylic composite.

Yet, limitations remain when it comes to the quantitative characterisation of composite constituents with AFM. Most of them are similar to those encountered in DSI (see Section 2), though the impact on measurement accuracy is much more localised in AFM. First, measurement artefacts may lead to an overestimation of the modulus close to the fibre-polymer interface [64, 66–69]. As observed in DSI, the tip may either hit the fibre (“probe effect”) or sense the influence from the fibre (“fibre bias”) while indenting the matrix, which may mask the intrinsic

interphase behaviour. FE modelling of the AFM indentation experiment has been performed for several composite systems in order to quantify the influence of these effects on modulus calculation [64, 66–69]. In all cases, the impact of the fibre bias and probe effects on modulus values were limited to the first tenths of nanometres of the interphase region, see Figure 3c. The corresponding modulus values were either corrected using FEA [64, 67–69] or discarded [66]. These studies also revealed a dependency of the impacted zone size upon various factors, e.g. matrix and reinforcement moduli, peak load value and nominal radius of the AFM tip [66, 68]. Note that, in general, the size of the interaction volume in AFM (i.e. the size of the zone mechanically affected by the contact with the tip) conditions both the spatial resolution and sensitivity of the mechanical measurements [70, 76]. It should be adjusted depending on the purpose of the AFM experiment, knowing that a larger interaction volume tends to improve the property contrast and accuracy of the mechanical mapping at the expense of spatial resolution [70].

Finally, sample preparation for AFM analysis of composite surfaces is more challenging than for DSI, as surface roughness interferes even more strongly with measurement accuracy [58, 66, 77]. In particular, differential erosion between the reinforcement and matrix materials should be mitigated during the polishing step [66]. As shown in Figure 3c, differences in height up to 150 nm between the fibres and the matrix are commonly observed on composite surfaces studied by AFM, and these are generally not accounted for when interpreting results or performing FE simulations of the experiment [62, 69]. Yet, an abrupt variation in surface slope at the fibre-matrix boundary could induce artefacts in the topographic image [77] and lead to erroneous modulus values close to the fibre surface as the tip-surface contact area does not actually correspond to the one assumed by the model used to extract the mechanical properties. Proposed solutions to limit differential erosion during preparation include ion milling [66], and the replacement of polishing pastes with diamond lapping films.

Over the past twenty years, composite interphases have been extensively characterised using semi-quantitative nanoscale techniques such as AFM. Interphase thickness and mechanical properties appear to strongly depend upon the type of fibre and fibre sizing used for composite manufacturing. Hence, interphase thickness may vary from a few nanometres for unsized fibres [78, 79], to 20–500 nm for sized carbon fibres [78–81]) and even up to 0.5–10 μm for sized glass fibres [58, 62, 65, 82–85]. Some interphases appear more compliant than the matrix material (possibly due to the preferential adsorption of certain resin components onto the fibre surface) [58, 78, 81, 83, 85], while others demonstrate intermediate response with respect to the fibre and matrix materials [69, 79, 84].

4. In situ mechanical testing in SEM coupled to DIC

Digital image correlation (DIC) is a non-contact optical method that allows tracking displacements over the deformed surface of a material. The principle relies on a correlation process using the grey level intensity of subsets of a pattern present on the material surface, each being unique, and distanced by a certain subset spacing [9, 86, 87], see Figure 4a. The pattern can either result from surface features inherent to the material (e.g. fibres in composites) or from deposition of small particles, resulting in a speckle pattern. At the macro and mesoscales, DIC is a popular technique to characterise the deformation of materials, including fibre-reinforced composites (FRPs) [11–13, 88]. Recently, DIC has also been applied at the microscale, combined with in-situ testing within a scanning electron microscope (SEM), to quantitatively investigate deformation and fracture processes. However, the use of micro-DIC in the study of FRPs remains limited due to practical challenges, encompassing equipment limitations (in-situ testing in a SEM),

cumbersome specimen preparation (machining, polishing, speckle pattern deposition) and limitations directly related to DIC itself and to the process of image acquisition (noise, image distortion, polymer relaxation during interrupted tests) [89–91]. In bottom-up multiscale approaches, the current micromechanical analyses on representative volume elements (RVE) at the ply level essentially rely on matrix models, which are identified and validated at the macroscale on pure polymer specimens. Additionally, fibre-matrix interface properties used in FEA often lack experimental validation. Hence, micro-DIC is particularly relevant to challenge the validity of existing models at the constituent level, and to improve the accuracy of the FE predictions at the microscale, with direct impact on the predictive capabilities of multiscale approaches regarding the macroscopic properties.

Canal et al. [92] first demonstrated the potential of micro-DIC for analysing FRPs by studying the deformation mechanisms of a unidirectional (UD) E-glass/epoxy composite subjected to transverse compression inside a SEM. At high magnifications, DIC qualitatively matched with the displacement and strain fields over the region of interest (ROI) simulated by a FEA relying on an elastic material behaviour. Strain localisation within small inter-fibre matrix ligaments were also detected by DIC. Still, the average strains in each phase could not properly be quantified, as DIC strains were under- and overestimated in the matrix and fibres, respectively, due to smoothing in the correlation process at the fibre-matrix interface. The conclusion of this work was that DIC can accurately determine the average composite strain over the ROI, but not at the individual phase level.

Following the work of Canal et al. [92], Mehdikhani et al. [93] studied a UD glass fibre/epoxy composite loaded in-situ in transverse three-point bending, focusing the ROI in the zone of tensile deformation. They showed the importance of evaluating the errors related to micro-DIC, such as speckle pattern quality, DIC parameters or charging effect of the fibres to ensure a quantitative data, see Figure 4c. They accurately mapped the displacement and strain fields with DIC, when compared to FEA maps considering an elastic matrix. The DIC maps also helped to identify the regions subject to strain concentration, but failed to capture large strain variations in confined spaces, such as in-between two close fibres (still due to smoothing). A subsequent study by Mehdikhani et al. [94] showed that, using a high-quality speckle pattern, highly accurate displacement and strain maps could be measured in hierarchical fibre-reinforced composites (using carbon nanotubes (CNTs)), enabling the observation of debonding and CNT clusters.

Recent advances in the speckle pattern deposition allow producing consistent and controlled nanoscale patterns using simple methods, such as physical vapour deposition or multi-layer sputtering [95,96]. Additionally, improvements of the image correlation algorithms provide more information on the initiation and evolution of fibre-matrix decohesion [97].

Ultimately, these studies illustrate the enormous potential of micro-DIC for studying the individual behaviour of FRPs constituents. Based on the aforementioned developments, and driven by the inability of micromechanical analyses using a validated model for the matrix [51] to reproduce transverse compression experimental results (i.e. matrix dominated composite response), the more complex case of matrix plasticity at the scale of the fibres was also addressed [49,98]. In-situ transverse compression tests performed on notched UD specimens in a SEM enabled direct observation of strain localisation and cracking in the matrix at the microscale. FE models, built from the ROI microstructures (and subjected to boundary conditions determined by the DIC displacement field), were used to confront the experimental and simulated strain fields. The FE maps generated using the macroscopic model of the matrix managed to reproduce the strain field in larger matrix pockets, away from the constraint of close fibres. Reversely, in more confined areas, FEA significantly under- or overestimated the strain field measured by DIC. In the former case, the very high DIC strain amplitudes in the localisation band could be predicted by the model only when suppressing the large strain re-hardening stage in the constitutive law, see

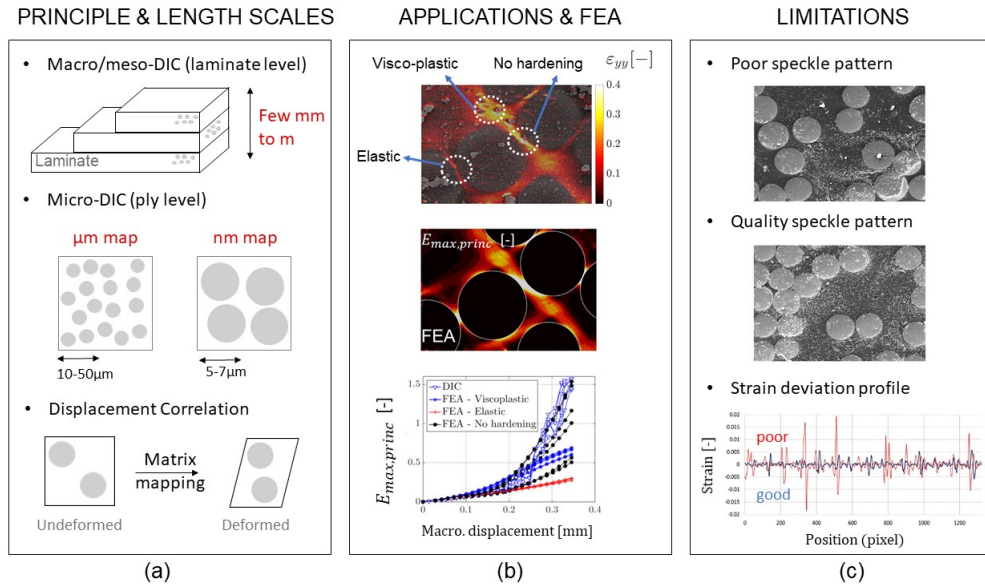


Figure 4. Digital image correlation applied to polymer-based composites; (a) length scales at play; (b) example of a carbon fibre-reinforced RTM6 composite [49]; (c) challenge related to speckle quality [93].

Figure 4b. In the latter case, no significant strain localisation was observed by DIC in several areas close to fibres, in disagreement with the model predictions. The key conclusion from these results is the inability of a macroscopic model - that averages the lower scale deformation and damage mechanisms in the matrix into a single continuum constitutive law - to accurately capture a microscale mechanical behaviour guided by local heterogeneities, which are either (1) inherent to the material itself, (2) related to processing conditions or (3) related to the “disturbing” presence of another constituent. Among other factors, this inability may be due to the absence of size effects in the constitutive model describing the matrix, or to a different material behaviour inside the interphase region.

5. Fibre push-out

In FRPs, the quality of the interface between the matrix and the fibres is key to ensure proper load transfer from the former to the latter, and thus to exploit the full potential of the fibres' high stiffness and high strength. Interfaces/interphases often constitute the locus of first damage in the composites [99–101]. The fibre-matrix decohesion not only reduces the ability of the fibres to carry the load, but debonded interfaces also become preferential sites for the initiation of additional damage mechanisms, i.e. transverse cracking, delamination or fibre kinking [102, 103]. Hence, the interfacial region has been the object of many studies, aiming both at understanding its mechanical behaviour and delaying the onset of decohesion. As a proof of the role played by the interfaces in the onset of damage in FRP, several authors reported an increase of the mechanical performance of FRPs at the coupon level with the improvement of the fibre-matrix interfacial adhesion (achieved by applying a chemical treatment called sizing to the surface of the fibres) [102–105]. However, macroscopic tests fail at directly identifying the intrinsic properties of this fibre-matrix interface. Even when the loading conditions aim at preferentially triggering the fibre-matrix decohesion mechanism (e.g. interlaminar shear tests), the results only provide an

indirect indication of the fibre-matrix bonding quality. The interface region is characterised by its own chemical and structural and properties, which are different from those of the fibres and the matrix. As a result, in micromechanical models, interfaces are usually incorporated as a third true constituent of the composite, with its own material law. Thus, direct measurement methods are heavily needed (1) to extract the necessary ingredients for micromechanical simulations (towards accurate modelling of the composite at the microscale), and (2) to develop a testing framework that would facilitate a direct quantitative comparison of interface properties as a function of, e.g., sizing type or ageing conditions.

In this respect, several experimental methods have been developed for the direct mechanical characterisation of fibre-matrix interface properties. Some of them rely on the manufacturing of a “model composite” consisting of a single fibre embedded in the polymer matrix, in particular the single fibre fragmentation test [102, 106], the micro-droplet test [107, 108], and the single fibre pull-out test [109, 110]. While these methods require careful specimen preparation, direct interface properties can be extracted based on simplifying assumptions about the stress state at the fibre-matrix interface. However, the main drawbacks of these experimental methods lie in their inability to reproduce the real environment of the interfaces within the composite. As a matter of fact, the interface properties depend on the processing conditions of the composite, which dictate the physical and chemical properties of the matrix (i.e. cross-linking density or crystallinity) and the build-up of thermal residual stresses [111–115] and are thus also dependent on the local microstructure (i.e. fibre volume fraction). Moreover, the strong dependence of the measured properties on the test set-up and test conditions are highlighted by the large scatter observed when comparing the results obtained on similar systems with different methods [116].

As a consequence, the fibre indentation/compression test methods have emerged as an attractive approach to locally extract the in-situ interface properties of the composite. A single interface is selected on the polished cross-section of a composite laminate and loaded using the tip of a nanoindenter. The fibre indentation tests are separated in two categories: the fibre push-in and the fibre push-out tests. The latter differs from the former by the requirement of carefully preparing thin slices of composite ($< 100 \mu\text{m}$ in thickness) so that the fibre is totally pushed out the specimen when the interface fails (see Figure 5a). Push-in tests do not require the same demanding specimen preparation, but the interpretation of the results does not profit from the conceptual simplicity of the push-out configuration [112]. The challenge to correctly execute and interpret push-out test results is two-fold. On the one hand, it relies on meticulous specimen preparation to produce material slices with controlled thickness and parallelism, as well as mirror-like polishing. The boundary conditions for the mechanical loading step must be chosen so as to reduce as much as possible the system compliance, ensuring the measurement of the true interface stiffness and strength. For instance, nickel or copper grids with $50 \times 50 \mu\text{m}^2$ wire spacing are appropriate to offer a rigid support to the specimens, while allowing the fibre to be effectively pushed out of the bottom surface. On the other hand, the analysis of the results is complex: the compliance of the set-up, the influence of the local environment (i.e. local fibre volume fraction) as well as the different energy-dissipating contributions must be understood and accounted for [115].

Figure 5b shows examples of fibre push-out results obtained for the carbon fibre-RTM6 system. The magenta curves are representative of low fibre volume fraction areas and the black ones of densely packed regions. The load-displacement graph provides the overall response of the volume element, while the time-displacement curves highlight the displacement jump characteristic of final crack propagation at the interfaces. The curves also display a complex non-linear shape, combination of matrix plasticity, crack initiation and propagation as well as friction. Experimental procedures like the cyclic push-out test can help decipher the importance of each contribution to the test response [116]. Still, while these methods are necessary to improve the

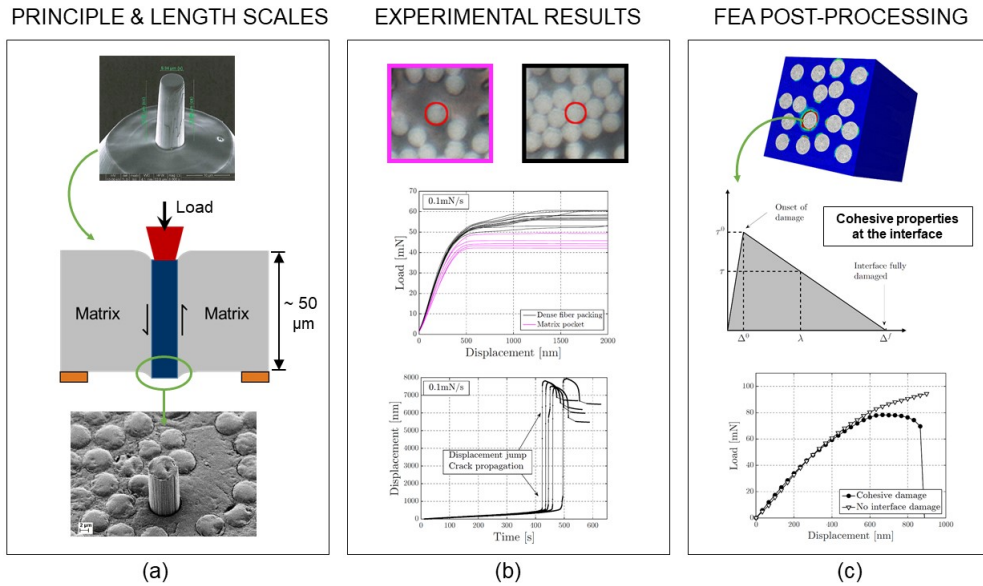


Figure 5. Push out test applied to polymer-based composites: (a) micrograph of a typical nanoindenter flat tip, schematic representation of the single fibre push-out test and micrograph of a debonded fibre at the end of a test; (b) micrograph showing indented fibres with different surrounding configurations, load-displacement curves resulting from fibre push-out tests and time-displacement curves showing the displacement jump characteristic of final crack propagation; (c) 3D finite element simulation of a push-out test (equivalent plastic strain in the matrix), typical bi-linear stress-displacement law for cohesive zones, load-displacement curves from FEA with and without damage at the interface.

understanding of the sequence of events, FEA is always needed to extract the interface properties. The post-processing of the results using FEA requires a careful understanding of the properties that need to be implemented in the cohesive-zone models, which are the standard nowadays for modelling interfaces, see Figure 5c. Indeed, as reviewed in earlier sections, modelling the microscale behaviour of composite materials faces challenges related to the possible different behaviour of the matrix at the microscale with respect to the macroscopic one, and to the presence of an interphase region with unknown properties. Friction effects have already been successfully incorporated into interface models [98, 117], but it remains to be determined if all local effects must be included in the cohesive-zone models. To the authors' knowledge, there is still no consensus on the best practices to extract traction-separation laws from single fibre push-out tests.

6. Mesoscale modelling via shear transformation zone (STZ) dynamics

The local large deformation response of the polymer matrix can play a primordial role in the macroscopic deformation and failure behaviour of a FRP composite laminate. Classical methods to simulate a laminate's behaviour rely on a bottom-up multiscale modelling approach where the simulated constitutive behaviour at a certain length scale (e.g. fibre diameter) is transferred to a larger length scale of interest (e.g. ply thickness) via homogenisation techniques [118]. An ongoing challenge is to realistically model the inelastic deformation of the polymer matrix at a length scale corresponding to the distance between the fibres (i.e. $0.1 \mu\text{m}$ to $10 \mu\text{m}$).

This is, as shown in Section 4, the relevant length scale at where intense localisation of the polymer via shear banding is observed [27, 119, 120] followed or cooperating with damage and interface cracking. On the one hand, one can make use of atomistic simulations such as (coarse-grained) molecular dynamic (MD) simulations. These provide insight into the fundamental deformation mechanisms dictating the polymer's (visco)plastic deformation. However, due to the high demand in computational power, constitutive MD models for polymers are typically restricted to domain sizes in the order of 10 to 100 nm [121] and very short time scales. On the other hand, there is a large amount of sophisticated (visco)elastic-(visco)plastic continuum frameworks to predict the complex large deformation response of glassy polymers [122–127]. These models give good agreement to measured uniaxial stress-strain curves obtained via tests on bulk specimens. However, they rely on a large number of largely phenomenological calibration parameters, and model predictions for the deformation behaviour of the matrix at the scale of the fibres have rarely been compared with micro-scale measurements, see [98, Section 4].

Mesoscale computational models based on STZ dynamics offer a practical avenue to bridge typical simulation length scales of molecular dynamics and continuum models. The STZ framework was originally developed by Argon [128, 129] to predict the viscoplastic response of metallic glasses. The theory assumes that the macroscopic inelastic deformation of an amorphous material at a temperature T close to but below the glass transition temperature T_g is dictated by thermally-activated local shear deformations of small material volumes. The attempt rate for transformation of an individual STZ is calculated via transition state theory, where the activation energy barrier is calculated via Eshelby's inclusion theory. Due to elastic interaction with the surrounding matrix, the activation of an STZ may increase the probability for a neighbouring STZ to transform. The resulting avalanche of sessile STZ activations may lead to localised flow in the form of shear bands, which may ultimately lead to material failure. Extensive numerical [130–135] and some indirect experimental [136–138] evidence exists for the inelastic deformation of metallic and polymeric glasses at $T/T_g < 1$ (and at moderate strain rates) to be governed by STZ dynamics.

Recently, the UCLouvain team extended the mesoscale FE model developed by Homer and Schuh [139–142] based on Argon's STZ theory [128, 143] to predict the viscoplastic deformation behaviour of polymeric glasses [120]. In brief, a linear elastic polymer matrix domain is discretised into a plane strain triangular mesh. Each element forms an STZ in combination with its neighbouring (node-sharing) elements, see Figure 6a. The average stress state of each STZ is calculated at the start of an increment by solving the boundary value problem of an STZ-enriched polymer matrix with an FE solver. The activation attempt rate of each STZ during this increment is dictated by the competition between mechanical energy provided by the homogenised stress state and the free energy barrier ΔF for the deformation of the STZ within the elastic matrix, see Figure 6b. The value of ΔF is calculated via Eshelby's inclusion theory following Argon's approach [128, 129, 144]. We have modified this energy barrier calculation for the case of polymeric glasses; details are included in the work of Chevalier et al. [120]. A Monte Carlo method is used to select the STZs that are activated within the increment. Selected STZs are subjected to a pure shear eigenstrain γ_0 in the direction of the maximum in-plane resolved shear stress and the FE solver is used to compute the simulated domain's equilibrium stress and strain state for the next increment. The STZ model requires the calibration of only five parameters to predict the uniaxial stress-strain response of a glassy polymer including the yield, softening, and hardening regime [120]. Due to the simulated heterogeneous nature of the inelastic deformation, the framework provides insight into typical phenomena observed in the large deformation response of polymers including the non-linear unloading behaviour, the Bauschinger effect, as well as rejuvenation/ageing. In addition, model predictions can be used to study the nucleation and growth of micro-sized shear bands in a deformed polymer matrix when confined by stiff fibres. This is

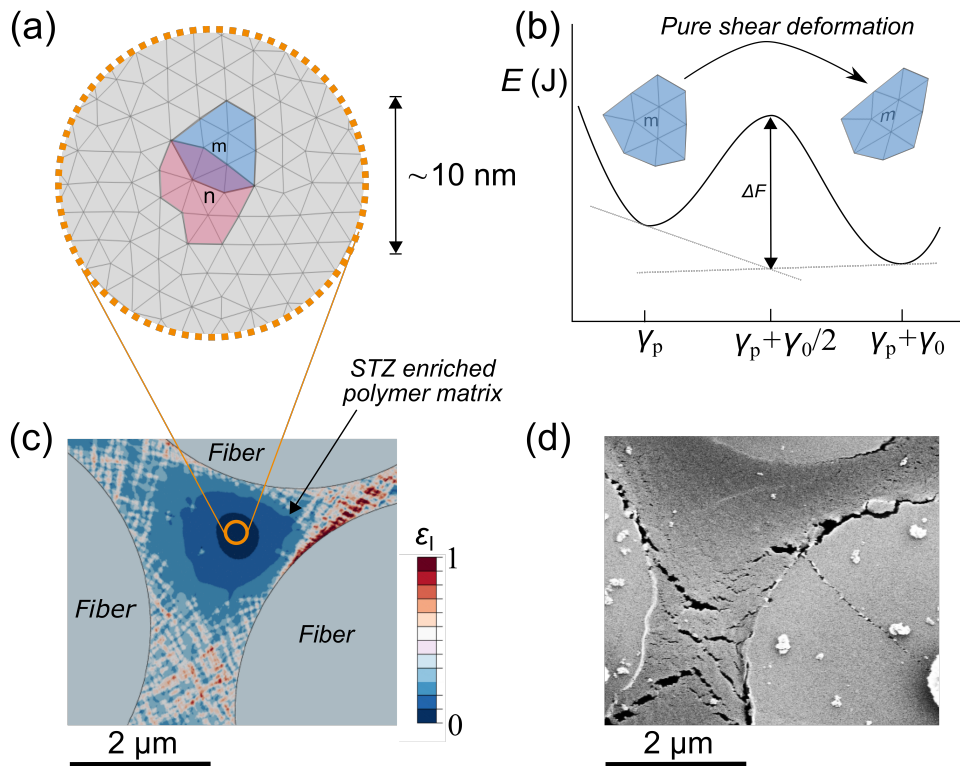


Figure 6. STZ approach applied to polymers. (a) Finite element mesh of the polymer matrix domain and illustration of the STZ assignment scheme: each element forms an STZ together with its node-sharing elements. (b) Illustration of the simplified energy landscape for deformation of an STZ in pure shear (via an eigenstrain of magnitude γ_0). (c) Predicted contours of constant maximum principle strain ϵ_I on a unidirectional fibre-matrix RVE in displacement-controlled transverse compression; the applied displacements on the RVE boundaries give an homogenised strain state equal to the homogenised strain state on a region of a SEM image (d) taken during transverse compression of a unidirectional carbon fibre-epoxy ply.

shown in Figure 6c, where predicted contours of constant maximum principle strain ϵ_I are shown for a unidirectional fibre-matrix RVE loaded in transverse compression. The predicted distribution, orientation and width of the shear bands is in relatively good agreement with those observed on in-situ SEM micrographs of a carbon fibre-epoxy ply loaded in transverse compression, see Figure 6d, while standard continuum modelling approaches fail to predict this micro-sized shear band network as explained earlier [98]. In-situ SEM micrographs of transversally compressed UD composites also indicate that microcracks nucleate and grow along the sites of the localised shear-band type inelastic flow in the polymer matrix, see Figure 6d. Hence, the extension of the STZ model could potentially be used to study the failure of the composite material by simulating the complex interaction between matrix-fibre interfacial fracture and damage in the matrix due to intense shear localisation.

Despite the promising outlook, the use of STZ dynamics for the mesoscale modelling of the large strain, inelastic constitutive behaviour of polymer glasses (and composites made thereof) is still in its infancy. We conclude by identifying some challenges and opportunities. One avenue of

future research includes the relation between the heterogeneous structural nature of the polymer on the molecular scale and the STZ activation dynamics [145]. As discussed in Section 3, AFM provides a powerful tool to probe the properties of a polymer matrix at the nano-scale. These measurements indicate that (1) the elastic field landscape of an undeformed, fully cured epoxy can be heterogeneous on the length scale corresponding to several STZs [54,120] and (2) property gradients in the matrix close to the sizing-coated fibres exist. The effect of these phenomena on the degree of localisation (and failure) of the deformed matrix close to the fibre is an excellent case study for an STZ-enriched mesoscale model. From a more practical point of view, the sensitivity of the model response to the values of its basic ingredients (e.g., the value of the activation eigenstrain γ_0 and of the activation volume) should be explored in more detail. This could provide a sound basis for the calibration of an STZ-based mesoscale model for a material system of interest. This calibration is typically guided by atomistic simulations (to provide, e.g., a physical range for the value of γ_0) and uniaxial deformation tests on macro-sized samples and/or (nano)indentation tests on small material volumes (to provide, e.g., a range for the activation volume). However, the final selection of the values of these fundamental parameters often remains a somewhat arbitrary stress-strain curve fitting task to date. Lastly, we note that for elevated temperatures close to T_g , the viscoelastic response of the polymer matrix may play a role in the cooperative organisation of activated STZs into shear bands. The role of viscoelastic matrix relaxation upon STZ activation should be explored in more detail too.

7. Conclusion and perspectives

Four different nanomechanical testing techniques – nanoindentation, AFM, SEM-DIC, fibre push in/out – and one mesoscale model based on STZ activation dynamics have been reviewed in the context of a quantitative description of the local fibre-matrix response of polymer-based composites. Experimental and modelling results on a highly cross-linked epoxy resin (RTM6) reinforced by CF have been highlighted to illustrate the methods but also to deliver the current state of understanding of the mechanisms in this reference system. These results confirm that although a qualitative description of the mechanical behaviour can be obtained with classical continuum models, yet many questions remain regarding the quantitative prediction of the viscoplastic, shear banding and damage processes as related to the unknown precise nature/structure of the material and interphase at the local fibre-matrix length scale.

Specific conclusions regarding each method have been provided inside each section. As a general conclusion, it is essential to acknowledge that a combination of several of these methods is needed to generate the full picture and shed light on the aforementioned issues, for instance:

- The interphase and confined matrix response (and thus AFM, nanoindentation and a STZ-inspired mesoscale model) are needed to simulate the push-out test data and identify, by inverse modelling, accurate interface properties;
- But, these interface failure properties are needed to simulate the in-situ SEM compression tests until fracture and make a quantitative comparison with DIC data;
- The STZ model could be used to identify the parameters of a coarse-grained cohesive law for the interface region between the fibre and the matrix. This cohesive law can be used in a continuum finite element model of a representative volume element of the composite. To this end, an intrinsic traction-separation law for the interface should be combined with an STZ mesoscale model that explicitly takes the interphase region surrounding the fibre into account.

As indicated in the last example, challenges on scale transition methods in order to coarse grain information from the sub-micrometre length scale also exist to properly account for the

impact of these lower scale effects at the macroscopic level. Another important element not addressed in the paper is related to the damage and fracture mechanisms in bulk resins, which are known to be dominated by defects in the range of micrometres to tens of micrometres. Such defects are not seen as dominating the matrix failure at fibre-confined matrix level, and care should thus be taken not to extend, again, bulk data (for instance macroscopic fracture strains) to the local level. Another important subject that could benefit from nanoscale investigation concerns the ageing mechanisms taking place at the interface/interphase levels, and that could be locally investigated by the methods above in order to develop less phenomenological ageing-induced damage models.

Finally, the extensive list of approaches described and analysed in this paper is far from being comprehensive. Atomistic simulations, x-ray synchrotron computed tomography (CT), micro fibre pull-out or micropillar compression are among the other methods available that could enrich the understanding of the local fibre-matrix response. In particular, in situ x-ray CT already mentioned in the introduction [6–8, 146] provide invaluable information on the sequence of damage events and interplay between failure mechanisms. For instance, Breite et al. [147] very recently addressed interactions effects between fiber breaks at local cluster level using ultrafast synchrotron CT scans, and Ni et al. [148], using the same technique, studied the effects of nanoscale interlaminar reinforcement on the damage progression in double-edge notched composite laminates. With the increasing resolution of synchrotron based tools one can progressively look at deformation and fracture phenomena at submicron scale with these techniques relevant for the fibre-matrix elementary length scale. The combination with digital volume correlation method made possible by the dispersion of nanoscopic markers in the matrix is nowadays offering the holy grail of extracting local 3D deformation fields together with information on the failure process [149].

References

- [1] A. R. Melro, P. P. Camanho, F. M. Andrade Pires, S. T. Pinho, “Micromechanical analysis of polymer composites reinforced by unidirectional fibres: Part I – Constitutive modelling”, *Int. J. Solids Struct.* **50** (2013), no. 11-12, p. 1897-1905.
- [2] A. R. Melro, P. P. Camanho, F. M. Andrade Pires, S. T. Pinho, “Micromechanical analysis of polymer composites reinforced by unidirectional fibres: Part II – Micromechanical analyses”, *Int. J. Solids Struct.* **50** (2013), no. 11-12, p. 1906-1915.
- [3] Y. Liu, F. P. Meer, L. J. Van der Sluys, J. T. Fan, “A numerical homogenization scheme used for derivation of a homogenized viscoelastic-viscoplastic model for the transverse response of fiber-reinforced polymer composites”, *Compos. Struct.* **252** (2020), article no. 112690.
- [4] Z. Liu, M. A. Bessa, W. K. Liu, “Self-consistent clustering analysis: An efficient multi-scale scheme for inelastic heterogeneous materials”, *Comput. Methods Appl. Mech. Eng.* **306** (2016), p. 319-341.
- [5] R. Bedzra, S. Reese, J.-W. Simon, “Hierarchical multi-scale modelling of flax fibre/epoxy composite by means of general anisotropic viscoelastic-viscoplastic constitutive models: Part I – Micromechanical model”, *Int. J. Solids Struct.* **202** (2020), p. 299-318.
- [6] R. Kopp, X. Ni, E. Kalfon-Cohen, C. Furtado, A. Arteiro, G. Borstnar, M. Mavrogordato, L. Helfen, I. Sinclair, S. M. Spearing, P. Camanho, B. L. Wardle, “Damage micro-mechanisms in notched hierarchical nanoengineered thin-ply composite laminates studied by in-situ synchrotron X-ray microtomography”, in *AIAA Scitech 2019 Forum*, American Institute of Aeronautics and Astronautics, 2019.
- [7] S. C. Garcea, I. Sinclair, S. M. Spearing, P. J. Withers, “Mapping fibre failure in situ in carbon fibre reinforced polymers by fast synchrotron X-ray computed tomography”, *Compos. Sci. Technol.* **149** (2017), p. 81-89.
- [8] E. Schöberl, C. Breite, A. Melnikov, Y. Swolfs, M. N. Mavrogordato, I. Sinclair, S. M. Spearing, “Fibre-direction strain measurement in a composite ply under quasi-static tensile loading using Digital Volume Correlation and in situ Synchrotron Radiation Computed Tomography”, *Compos. Part A Appl. Sci. Manuf.* **137** (2020), article no. 105935.
- [9] M. Bornert, F. Brémand, P. Doumalin, J.-C. Dupré, M. Fazzini, M. Grédiac, F. Hild, S. Mistou, J. Molimard, J.-J. Orteu, L. Robert, Y. Sirel, P. Vacher, B. Wattrisse, “Assessment of Digital Image Correlation Measurement Errors: Methodology and Results”, *Exper. Mech.* **49** (2009), p. 353-370.

- [10] A. Buljac, C. Jailin, A. Mendoza, J. Neggers, T. Taillandier-Thomas, A. Bouterf, B. Smaniotto, F. Hild, S. Roux, "Digital Volume Correlation: Review of Progress and Challenges", *Exp. Mech.* **58** (2018), p. 661-708.
- [11] G. Catalanotti, P. P. Camanho, J. Xavier, C. G. Dávila, A. T. Marques, "Measurement of resistance curves in the longitudinal failure of composites using digital image correlation", *Compos. Sci. Technol.* **70** (2010), no. 13, p. 1986-1993.
- [12] S. V. Lomov, D. S. Ivanov, I. Verpoest, M. Zako, T. Kurashiki, H. Nakai, J. Molimard, A. Vautrin, "Full-field strain measurements for validation of meso-FE analysis of textile composites", *Compos. Part A Appl. Sci. Manuf.* **39** (2008), no. 8, p. 1218-1231.
- [13] M. Zhu, L. Gorbatikh, S. Fonteyn, D. Van Hemelrijck, L. Pyl, D. Carrella-Payan, S. V. Lomov, "Digital image correlation assisted characterization of Mode I fatigue delamination in composites", *Compos. Struct.* **253** (2020), article no. 112746.
- [14] I. B. C. M. Rocha, P. Kerfriden, F. P. v. d. Meer, "Micromechanics-based surrogate models for the response of composites: A critical comparison between a classical mesoscale constitutive model, hyper-reduction and neural networks", *Eur. J. Mech. - A Solids* **82** (2020), article no. 103995.
- [15] M. A. Bessa, R. Bostanabad, Z. Liu, A. Hu, D. W. Apley, C. Brinson, W. Chen, W. K. Liu, "A framework for data-driven analysis of materials under uncertainty: Countering the curse of dimensionality", *Comput. Methods Appl. Mech. Eng.* **320** (2017), p. 633-667.
- [16] S. Tang, Y. Li, H. Qiu, H. Yang, S. Saha, S. Mojmudar, W. K. Liu, X. Guo, "MAP123-EP: A mechanistic-based data-driven approach for numerical elastoplastic analysis", *Comput. Methods Appl. Mech. Eng.* **364** (2020), no. 1, article no. 112955.
- [17] N. A. Fleck, J. W. Hutchinson, "A reformulation of strain gradient plasticity", *J. Mech. Phys. Solids* **49** (2001), no. 10, p. 2245-2271.
- [18] D. C. C. Lam, A. C. M. Chong, "Indentation model and strain gradient plasticity law for glassy polymers", *J. Mater. Res.* **14** (1999), no. 9, p. 3784-3788.
- [19] J. Chevalier, X. P. Morelle, P. P. Camanho, F. Lani, T. Pardoen, "On a unique fracture micromechanism for highly cross-linked epoxy resins", *J. Mech. Phys. Solids* **122** (2019), p. 502-519.
- [20] T. Hobbiebrunken, B. Fiedler, M. Hojo, M. Tanaka, "Experimental determination of the true epoxy resin strength using micro-scaled specimens", *Compos. Part A Appl. Sci. Manuf.* **38** (2007), no. 3, p. 814-818.
- [21] J. Misumi, R. Ganesh, S. Sockalingam, J. W. Gillespie, "Experimental characterization of tensile properties of epoxy resin by using micro-fiber specimens", *J. Reinf. Plast. Compos.* **35** (2016), no. 24, p. 1792-1801.
- [22] X. Sui, M. Tiwari, I. Greenfeld, R. L. Khalfin, H. Meeuw, B. Fiedler, D. H. Wagner, "Extreme scale-dependent tensile properties of epoxy fibers", *Express Polym. Lett.* **11** (2019), no. 13, p. 993-1003.
- [23] O. Verschate, L. Daelemans, W. Van Paeppegem, K. De Clerck, "In-situ observations of microscale ductility in a quasi-brittle bulk scale epoxy", *Polymers* **12** (2020), no. 11, article no. 2581.
- [24] C. Breite, A. Melnikov, A. Turon, A. B. de Moraes, F. Otero, F. Mesquita, J. Costa, J. A. Mayugo, J. M. Guerrero, L. Gorbatikh, L. N. McCartney, M. Hajikazemi *et al.*, "Blind benchmarking of seven longitudinal tensile failure models for two virtual unidirectional composites", *Compos. Sci. Technol.* (2020), article no. 108555.
- [25] C. Breite, A. Melnikov, A. Turon, A. B. de Moraes, C. Le Bourlot, E. Maire, E. Schöberl, F. Otero *et al.*, "Detailed experimental validation and benchmarking of six models for longitudinal tensile failure of unidirectional composites", submitted to *Composites Part A: Applied Science and Manufacturing*, 2020.
- [26] M. Hardiman, T. J. Vaughan, C. T. McCarthy, "A review of key developments and pertinent issues in nanoindentation testing of fibre reinforced plastic microstructures", *Compos. Struct.* **180** (2017), p. 782-798.
- [27] C. González, J. LLorca, "Mechanical behavior of unidirectional fiber-reinforced polymers under transverse compression: Microscopic mechanisms and modeling", *Compos. Sci. Technol.* **67** (2007), no. 13, p. 2795-2806.
- [28] F. Alisafaei, C.-S. Han, N. Lakhera, "Characterization of indentation size effects in epoxy", *Polym. Test.* **40** (2014), p. 70-78.
- [29] C.-S. Han, S. H. R. Sanei, F. Alisafaei, "On the origin of indentation size effects and depth dependent mechanical properties of elastic polymers", *J. Pol. Eng.* **36** (2016), p. 103-111.
- [30] W. C. Oliver, G. M. Pharr, "An improved technique for determining hardness and elastic modulus using load and displacement sensing indentation experiments", *J. Mater. Res.* **7** (1992), no. 6, p. 1564-1583.
- [31] I. N. Sneddon, "The relation between load and penetration in the axisymmetric Boussinesq problem for punch of arbitrary profile", *Int. J. Eng. Sci.* **3** (1965), no. 1, p. 47-57.
- [32] J. L. Loubet, M. Bauer, A. Tonck, S. Bec, B. Gauthier-Manuel, "Nanoindentation with a surface force apparatus", in *Mechanical properties and deformation behavior of materials having ultra-fine microstructures* (M. Nastasi, D. M. Parkin, H. Gleiter, eds.), NATO ASI Series, vol. 233, Springer, 1993, p. 429-447.
- [33] M. R. VanLandingham, J. S. Villarrubia, W. F. Guthrie, G. F. Meyers, "Nanoindentation of polymers: an overview", *Macromol. Symp.* **167** (2001), p. 15-43.
- [34] D. Tranchida, S. Piccarolo, J. Loos, A. Alexeev, "Accurately evaluating Young's modulus of polymers through nanoin-

- dentations: A phenomenological correction factor to the Oliver and Pharr procedure", *Appl. Phys. Lett.* **89** (2006), article no. 171905.
- [35] M. Hardiman, T. J. Vaughan, C. T. McCarthy, "The effects of pile-up, viscoelasticity and hydrostatic stress on polymer matrix nanoindentation", *Polym. Test.* **52** (2016), p. 157-166.
- [36] R. Martinez, L. R. Xu, "Comparison of the Young's moduli of polymers measured from nanoindentation and bending experiments", *MRS Commun* **4** (2014), no. 3, p. 89-93.
- [37] D. Tranchida, S. Piccarolo, J. Loos, A. Alexeev, "Mechanical characterization of polymers on a nanometer scale through nanoindentation. A study on pile-up and viscoelasticity", *Macromolecules* **40** (2007), no. 4, p. 1259-1267.
- [38] M. Rodríguez, J. M. Molina-Aldareguía, C. González, J. Llorca, "Determination of the mechanical properties of amorphous materials through instrumented nanoindentation", *Acta Mater.* **60** (2012), no. 9, p. 3953-3964.
- [39] A. C. M. Chong, D. C. C. Lam, "Strain gradient plasticity effect in indentation hardness of polymers", *J. Mater. Res.* **14** (1999), no. 10, p. 4103-4110.
- [40] G. Chandrashekar, C.-S. Han, "Length scale effects in epoxy: The dependence of elastic moduli measurements on spherical indenter tip radius", *Polym. Test.* **53** (2016), p. 227-233.
- [41] C.-S. Han, "Influence of the molecular structure on indentation size effect in polymers", *Mater. Sci. Eng. A* **527** (2010), no. 3, p. 619-624.
- [42] F. Alisafaei, C.-S. Han, "Indentation Depth Dependent Mechanical Behavior in Polymers", *Adv. Cond. Matter Phys.* **2015** (2015), article no. 391579.
- [43] W. Tan, F. Naya, L. Yang, T. Chang, B. G. Falzon, L. Zhan, J. M. Molina-Aldareguía, C. González, J. Llorca, "The role of interfacial properties on the intralaminar and interlaminar damage behaviour of unidirectional composite laminates: Experimental characterization and multiscale modelling", *Compos. Part B Eng.* **138** (2018), p. 206-221.
- [44] C. González, J. J. Vilatela, J. M. Molina-Aldareguía, C. S. Lopes, J. Llorca, "Structural composites for multifunctional applications: Current challenges and future trends", *Prog. Mater. Sci.* **89** (2017), p. 194-251.
- [45] J. Gregory, S. Spearing, "Nanoindentation of neat and polymers in polymer-matrix composites", *Compos. Sci. Technol.* **65** (2005), no. 3-4, p. 595-607.
- [46] M. Hardiman, T. J. Vaughan, C. T. McCarthy, "Fibrous composite matrix characterisation using nanoindentation: The effect of fibre constraint and the evolution from bulk to in-situ matrix properties", *Compos. Part A Appl. Sci. Manuf.* **68** (2015), p. 296-303.
- [47] M. Hardiman, T. J. Vaughan, C. T. McCarthy, "The effect of fibre constraint in the nanoindentation of fibrous composite microstructures: A finite element investigation", *Comput. Mater. Sci.* **64** (2012), p. 162-167.
- [48] Z. Hu, M. Farahikia, F. Delfanian, "Fiber bias effect on characterization of carbon fiber-reinforced polymer composites by nanoindentation testing and modeling", *J. Compos. Mater.* **49** (2015), no. 27, p. 3359-3372.
- [49] J. Chevalier, "Micromechanics of an epoxy matrix for fiber reinforced composites: experiments and physics-based modelling", PhD Thesis, Université Catholique de Louvain, France, 2018.
- [50] P. Frontini, S. Lotfian, M. A. Monclús, J. M. Molina-Aldareguia, "High temperature nanoindentation response of RTM6 epoxy resin at different strain rates", *Exp. Mech.* **55** (2015), p. 851-862.
- [51] X. P. Morelle, J. Chevalier, C. Bailly, T. Pardoën, F. Lani, "Mechanical characterization and modeling of the deformation and failure of the highly crosslinked RTM6 epoxy resin", *Mech. Time-Depend. Mater.* **21** (2017), p. 419-454.
- [52] G. Binnig, C. F. Quate, C. Gerber, "Atomic Force Microscope", *Phys. Rev. Lett.* **56** (1986), no. 9, p. 930-933.
- [53] S. A. Joyce, J. E. Houston, "A new force sensor incorporating force feedback control for interfacial force microscopy", *Rev. Sci. Instrum.* **62** (1991), p. 710-715.
- [54] A. Bahrami, X. Morelle, L. D. Hông Minh, T. Pardoën, C. Bailly, B. Nysten, "Curing dependent spatial heterogeneity of mechanical response in epoxy resins revealed by atomic force microscopy", *Polymer* **68** (2015), p. 1-10.
- [55] A. Bahrami, F. Cordenier, P. Van Velthem, W. Ballout, T. Pardoën, B. Nysten, C. Bailly, "Synergistic local toughening of high performance epoxy-matrix composites using blended block copolymer-thermoplastic thin films", *Compos. Part A Appl. Sci. Manuf.* **91** (2016), p. 398-405.
- [56] M. R. VanLandingham, S. H. McKnight, G. R. Palmese, T. A. Bogetti, R. F. Eduljee, J. W. Gillespie, "Characterization of interphase regions using atomic force microscopy", *MRS Proceedings* **458** (1996), article no. 313.
- [57] M. R. VanLandingham, R. R. Dagastine, R. F. Eduljee, R. L. McCullough, J. W. Gillespie, "Characterization of nanoscale property variations in polymer composite systems: 1. Experimental results", *Compos. Part A Appl. Sci. Manuf.* **30** (1999), no. 1, p. 75-83.
- [58] T. D. Downing, R. Kumar, W. M. Cross, L. Kjerengtroen, J. J. Kellar, "Determining the interphase thickness and properties in polymer matrix composites using phase imaging atomic force microscopy and nanoindentation", *J. Adhes. Sci. Tech.* **14** (2000), p. 1801-1812.
- [59] S. A. Syed Asif, K. J. Wahl, R. J. Colton, O. L. Warren, "Quantitative imaging of nanoscale mechanical properties using hybrid nanoindentation and force modulation", *J. Appl. Phys.* **90** (2001), p. 1192-1200.
- [60] S.-L. Gao, E. Mader, "Characterisation of interphase nanoscale property variations in glass fibre reinforced polypropylene and epoxy resin composites", *Compos. Part A Appl. Sci. Manuf.* **33** (2002), no. 4, p. 559-576.

- [61] J. M. He, Y. D. Huang, "AFM characterization of interphase properties of silver-coated carbon fibre reinforced epoxy composites", *Polym. Polym. Compos.* **14** (2006), no. 2, p. 123-134.
- [62] Y. Wang, T. H. Hahn, "AFM characterization of the interfacial properties of carbon fiber reinforced polymer composites subjected to hygrothermal treatments", *Compos. Sci. Technol.* **67** (2007), no. 1, p. 92-101.
- [63] S. Q. Wang, S. D. Nair, D. Hurley, S. H. Lee, "Characterizing interphase properties in fiber reinforced polymer composite with advanced AFM based tools", *Adv. Mater. Res.* **123–125** (2010), p. 403-406.
- [64] M. Qu, F. Deng, S. M. Kalkhoran, A. Gouldstone, A. Robisson, K. J. Van Vliet, "Nanoscale visualization and multiscale mechanical implications of bound rubber interphases in rubber-carbon black nanocomposites", *Soft Matter* **7** (2011), no. 3, p. 1066-1077.
- [65] V. Cech, E. Palesch, J. Lukes, "The glass fiber-polymer matrix interface/interphase characterized by nanoscale imaging techniques", *Compos. Sci. Technol.* **83** (2013), p. 22-26.
- [66] X. Cheng, K. W. Putz, C. D. Wood, L. C. Brinson, "Characterization of Local Elastic Modulus in Confined Polymer Films via AFM Indentation", *Macromol. Rapid Commun.* **36** (2015), no. 4, p. 391-397.
- [67] P. F. Brune, G. S. Blackman, T. Diehl, J. S. Meth, D. Brill, Y. Tao, J. Thornton, "Direct Measurement of Rubber Interphase Stiffness", *Macromolecules* **49** (2016), no. 13, p. 4909-4922.
- [68] M. Zhang, Y. Li, P. V. Kolluru, L. C. Brinson, "Determination of mechanical properties of polymer interphase using combined atomic force microscope (AFM) experiments and finite element simulations", *Macromolecules* **51** (2018), p. 8229-8240.
- [69] L. K. Babu, "The use of AFM indentation to quantify mechanical properties of the interphase region in fiber-reinforced composites", PhD Thesis, Oklahoma State University, USA, 2019.
- [70] A. Bahrami, C. Bailly, B. Nysten, "Spatial resolution and property contrast in local mechanical mapping of polymer blends using AFM dynamic force spectroscopy", *Polymer* **165** (2019), p. 180-190.
- [71] P. Maivald, H. J. Butt, S. A. C. Gould, C. B. Prater, B. Drake, J. A. Gurley, V. B. Elings, P. K. Hansma, "Using force modulation to image surface elasticities with the atomic force microscope", *Nanotechnology* **2** (1991), no. 2, p. 103-106.
- [72] M. Heuberger, G. Dietler, L. Schlapbach, "Mapping the local Young's modulus by analysis of the elastic deformations occurring in atomic force microscopy", *Nanotechnology* **6** (1995), no. 1, p. 12-23.
- [73] S. C. Minne, Y. Hu, S. Hu, B. Pittenger, C. Su, "Nanoscale quantitative mechanical property mapping using peak force tapping atomic force microscopy", *Microsc. Microanal.* **16** (2010), p. 464-465.
- [74] O. Sahin, S. Magonov, C. Su, C. F. Quate, O. Solgaard, "An atomic force microscope tip designed to measure time-varying nanomechanical forces", *Nat. Nanotechnol.* **2** (2007), p. 507-514.
- [75] J. A. Ramos, M. Blanco, I. Zalakain, I. Mondragon, "Nanoindentation study of interphases in epoxy/amine thermosetting systems modified with thermoplastics", *J. Colloid Interface Sci.* **336** (2009), no. 2, p. 431-437.
- [76] L. Belec, Y. Joliff, "Mechanically affected zone in AFM force measurements — Focus on actual probe tip geometry", *Mater. Des.* **104** (2016), p. 217-226.
- [77] P. Eaton, P. West, *Atomic Force Microscopy*, Oxford University Press, 2010.
- [78] T. A. Bogetti, T. Wang, M. R. VanLandingham, J. W. Gillespie, "Characterization of nanoscale property variations in polymer composite systems: 2. Numerical modeling", *Compos. Part A Appl. Sci. Manuf.* **30** (1999), no. 1, p. 85-94.
- [79] L. Liu, C. Jia, J. He, F. Zhao, D. Fan, L. Xing, M. Wang, F. Wang, Z. Jiang, Y. Huang, "Interfacial characterization, control and modification of carbon fiber reinforced polymer composites", *Compos. Sci. Technol.* **121** (2015), p. 56-72.
- [80] M. Munz, H. Sturm, E. Schulz, G. Hinrichsen, "The scanning force microscope as a tool for the detection of local mechanical properties within the interphase of fibre reinforced polymers", *Compos. Part A Appl. Sci. Manuf.* **29** (1998), no. 9-10, p. 1251-1259.
- [81] J. G. Williams, M. E. Donnellan, M. R. James, W. L. Morris, "Properties of the interphase in organic matrix composites", *Mater. Sci. Eng. A* **126** (1990), no. 1, p. 305-312.
- [82] R. M. Winter, J. E. Houston, "Interphase mechanical properties in an epoxy-glass fiber composite as measured by interfacial microscopy", in *Proceedings of the SEM Spring Conference on Experimental and Applied Mechanics and Experimental/Numerical Mechanics in Electronic Packaging III*, 1998, p. 355-358.
- [83] K. Mai, E. Mäder, M. Mühle, "Interphase characterization in composites with new non-destructive methods", *Compos. Part A Appl. Sci. Manuf.* **29** (1998), no. 9-10, p. 1111-1119.
- [84] Z. Boufaïda, "Analyse des propriétés mécaniques de composites taffetas verre/matrice acrylique en relation avec les propriétés d'adhésion des fibres sur la matrice", PhD Thesis, Université de Lorraine, France, 2015.
- [85] I. B. C. M. Rocha, S. Raijmakers, F. P. van der Meer, R. P. L. Nijssen, H. R. Fischer, L. J. Sluys, "Combined experimental/numerical investigation of directional moisture diffusion in glass/epoxy composites", *Compos. Sci. Technol.* **151** (2017), p. 16-24.
- [86] A. D. Kammers, S. Daly, "Digital image correlation under scanning electron microscopy: methodology and validation", *Exp. Mech.* **53** (2013), p. 1743-1761.
- [87] F. Lagattu, F. Bridier, P. Villechaise, J. Brillaud, "In-plane strain measurements on a microscopic scale by coupling digital image correlation and an in situ SEM technique", *Mater. Charact.* **56** (2006), no. 1, p. 10-18.

- [88] I. Miskdjian, M. Hajikazemi, W. Van Paepegem, "Automatic edge detection of ply cracks in glass fiber composite laminates under quasi-static and fatigue loading using multi-scale Digital Image Correlation", *Compos. Sci. Technol.* **200** (2020), article no. 108401.
- [89] J. R. Schreier, Hubert W. ans Braasch, M. A. Sutton, "Systematic errors in digital image correlation caused by intensity interpolation", *Opt. Eng.* **39** (2000), no. 11, p. 2915-2921.
- [90] M. Sutton, N. Li, D. Joy, A. Reynolds, X. Li, "Scanning Electron Microscopy for Quantitative Small and Large Deformation Measurements Part I: SEM Imaging at Magnifications from 200 to 10,000", *Exp. Mech.* **47** (2007), p. 775-787.
- [91] J. L. W. Carter, M. D. Uchic, M. J. Mills, "Impact of Speckle Pattern Parameters on DIC Strain Resolution Calculated from In-situ SEM Experiments", in *Fracture, Fatigue, Failure, and Damage Evolution, Volume 5* (J. Carroll, S. Daly, eds.), Conference Proceedings of the Society for Experimental Mechanics Series, Springer, 2015, p. 119-126.
- [92] L. P. Canal, C. González, J. M. Molina-Aldareguía, J. Segurado, J. LLorca, "Application of digital image correlation at the microscale in fiber-reinforced composites", *Compos. Part A Appl. Sci. Manuf.* **43** (2012), no. 10, p. 1630-1638.
- [93] M. Mehdikhani, M. Aravand, B. Sabuncuoglu, M. G. Callens, S. V. Lomov, L. Gorbatikh, "Full-field strain measurements at the micro-scale in fiber-reinforced composites using digital image correlation", *Compos. Struct.* **140** (2016), p. 192-201.
- [94] M. Mehdikhani, A. Matveeva, M. A. Aravand, B. L. Wardle, S. V. Lomov, L. Gorbatikh, "Strain mapping at the micro-scale in hierarchical polymer composites with aligned carbon nanotube grafted fibers", *Compos. Sci. Technol.* **137** (2016), p. 24-34.
- [95] J. P. M. Hoefnagels, M. P. F. H. L. van Maris, T. Vermeij, "One-step deposition of nano-to-micron-scalable, high-quality digital image correlation patterns for high-strain *in-situ* multi-microscopy testing", *Strain* **55** (2019), no. 6, article no. e12330.
- [96] C. B. Montgomery, B. Koohbor, N. R. Sottos, "A robust patterning technique for electron microscopy-based digital image correlation at sub-micron resolutions", *Exp. Mech.* **59** (2019), p. 1063-1073.
- [97] R. Naylor, C. Fagiano, M. Hirsekorn, B. Tranquart, E. Baranger, "Mesures de champs de déformations par corrélations d'images pour l'identification de modèles mécaniques microscopiques de composites à matrice polymère", in *Journées Nationales sur les Composites 2017*, Compte Rendus des JNC, vol. 17, École des Ponts ParisTech, 2017, p. 1-10.
- [98] J. Chevalier, P. P. Camanho, F. Lani, T. Pardoen, "Multi-scale characterization and modelling of the transverse compression response of unidirectional carbon fiber reinforced epoxy", *Compos. Struct.* **209** (2019), p. 160-176.
- [99] E. K. Gamstedt, B. A. Sjögren, "Micromechanisms in tension-compression fatigue of composite laminates containing transverse plies", *Compos. Sci. Technol.* **59** (1999), no. 2, p. 167-178.
- [100] T. Hobbiebrunken, M. Hojo, T. Adachi, C. De Jong, B. Fiedler, "Evaluation of interfacial strength in CF/epoxies using FEM and in-situ experiments", *Compos. Part A Appl. Sci. Manuf.* **37** (2006), no. 12, p. 2248-2256.
- [101] B. Harris, *Fatigue in composites: science and technology of the fatigue response of fibre-reinforced plastics*, Woodhead Publishing Limited, 2003.
- [102] M. S. Madhukar, L. T. Drzal, "Fiber-matrix adhesion and its effect on composite mechanical properties: I. Inplane and interlaminar shear behavior of graphite/epoxy composites", *J. Compos. Mater.* **25** (1991), no. 8, p. 932-957.
- [103] M. S. Madhukar, L. T. Drzal, "Fiber-matrix adhesion and its effect on composite mechanical properties: III. Longitudinal (0 degree) compressive properties of graphite/epoxy composites", *J. Compos. Mater.* **26** (1992), no. 3, p. 310-333.
- [104] B. K. Larson, L. T. Drzal, "Glass fibre sizing/matrix interphase formation in liquid composite moulding: effects on fibre/matrix adhesion and mechanical properties", *Composites* **25** (1994), no. 7, p. 711-721.
- [105] S. Subramanian, J. Lesko, K. Reifsnider, W. Stinchcomb, "Characterization of the fibre-matrix interphase and its influence on mechanical properties of unidirectional composites", *J. Compos. Mater.* **30** (1996), no. 3, p. 309-332.
- [106] J. Varna, R. Joffe, L. A. Berglund, "Interfacial toughness evaluation from the single-fiber fragmentation test", *Compos. Sci. Technol.* **56** (1996), no. 9, p. 1105-1109.
- [107] B. Miller, P. Muri, L. Rebenfeld, "A microbond method for determination of the shear strength of a fiber/resin interface", *Compos. Sci. Technol.* **28** (1987), p. 17-32.
- [108] F. Hoecker, J. Karger-Kocsis, "Effects of the interface on the mechanical response of CF/EP microcomposites and macrocomposites", *Composites* **25** (1994), no. 7, p. 729-738.
- [109] M. R. Piggott, S. R. Dai, "Fiber pull out experiments with thermoplastics", *Polym. Eng. Sci.* **31** (1991), no. 17, p. 1246-1249.
- [110] K. Tanaka, K. Minoshima, W. Grela, K. Komai, "Characterization of the aramid/epoxy interfacial properties by means of pull-out test and influence of water absorption", *Compos. Sci. Technol.* **62** (2002), no. 16, p. 2169-2177.
- [111] M. Desaege, I. Verpoest, "On the use of the micro-indentation test technique to measure the interfacial shear strength of fibre-reinforced polymer composites", *Compos. Sci. Technol.* **48** (1993), no. 1-4, p. 215-226.
- [112] M. Rodríguez, J. M. Molina-Aldareguía, C. González, J. LLorca, "A methodology to measure the interface shear strength by means of the fiber push-in test", *Compos. Sci. Technol.* **72** (2012), no. 15, p. 1924-1932.

- [113] J. Sha, J. Dai, J. Li, Z. Wei, J.-M. Hausherr, W. Krenkel, "Measurement and analysis of fiber-matrix interface strength of carbon fiber-reinforced phenolic resin matrix composites", *J. Compos. Mater.* **48** (2014), no. 11, p. 1303-1311.
- [114] M. Greisel, J. Jäger, J. Moosburger-Will, M. G. R. Sause, W. M. Mueller, S. Horn, "Influence of residual thermal stress in carbon fiber-reinforced thermoplastic composites on interfacial fracture toughness evaluated by cyclic single-fiber push-out tests", *Compos. Part A Appl. Sci. Manuf.* **66** (2014), p. 117-127.
- [115] J. Jäger, M. G. R. Sause, F. Burkert, J. Moosburger-Will, M. Greisel, S. Horn, "Influence of plastic deformation on single-fiber push-out tests of carbon fiber reinforced epoxy resin", *Compos. Part A Appl. Sci. Manuf.* **71** (2015), p. 157-167.
- [116] M. R. Piggott, "Why interface testing by single-fibre methods can be misleading", *Compos. Sci. Technol.* **57** (1997), no. 8, p. 965-974.
- [117] G. Alfano, E. Sacco, "Combining interface damage and friction in a cohesive-zone model: combining interface damage and friction in a cohesive-zone model", *Int. J. Numer. Meth. Eng.* **68** (2006), no. 5, p. 542-582.
- [118] J. Llorca, C. González, J. M. Molina-Aldareguía, J. Segurado, R. Seltzer, F. Sket, M. Rodríguez, S. Sádaba, R. Muñoz, L. P. Canal, "Multiscale Modeling of Composite Materials: a Roadmap Towards Virtual Testing", *Adv. Mater.* **23** (2011), no. 44, p. 5130-5147.
- [119] E. Totry, C. González, J. Llorca, J. M. Molina-Aldareguía, "Mechanisms of shear deformation in fiber-reinforced polymers: experiments and simulations", *Int. J. Fract.* **158** (2009), p. 197-209.
- [120] J. Chevalier, L. Brassart, F. Lani, C. Bailly, T. Pardoen, X. P. Morelle, "Unveiling the nanoscale heterogeneity controlled deformation of thermosets", *J. Mech. Phys. Solids* **121** (2018), p. 432-446.
- [121] T. E. Gartner, A. Jayaraman, "Modeling and Simulations of Polymers: A Roadmap", *Macromolecules* **52** (2019), no. 3, p. 755-786.
- [122] R. N. Haward, G. Thackray, "The use of a mathematical model to describe isothermal stress-strain curves in glassy thermoplastics", *Proc. Math. Phys. Eng. Sci.* **302** (1968), p. 453-472.
- [123] M. C. Boyce, D. M. Parks, A. S. Argon, "Large inelastic deformation of glassy polymers. part I: rate dependent constitutive model", *Mech. Mater.* **7** (1988), no. 1, p. 15-33.
- [124] C. Buckley, "Glass-rubber constitutive model for amorphous polymers near the glass transition", *Polymer* **36** (1995), no. 17, p. 3301-3312.
- [125] E. T. J. Klompen, T. A. P. Engels, L. E. Govaert, H. E. H. Meijer, "Modeling of the Postyield Response of Glassy Polymers: Influence of Thermomechanical History", *Macromolecules* **38** (2005), p. 6997-7008.
- [126] J. Johnsen, A. H. Clausen, F. Grytten, A. Benallal, O. S. Hopperstad, "A thermo-elasto-viscoplastic constitutive model for polymers", *J. Mech. Phys. Solids* **124** (2019), p. 681-701.
- [127] V. Srivastava, S. A. Chester, N. M. Ames, L. Anand, "A thermo-mechanically-coupled large-deformation theory for amorphous polymers in a temperature range which spans their glass transition", *Int. J. Plast.* **26** (2010), no. 8, p. 1138-1182.
- [128] A. S. Argon, "Plastic deformation in metallic glasses", *Acta Metall.* **27** (1979), no. 1, p. 47-58.
- [129] A. S. Argon, L. T. Shi, "Development of visco-plastic deformation in metallic glasses", *Acta Metall.* **31** (1983), no. 4, p. 499-507.
- [130] M. L. Falk, J. S. Langer, "Dynamics of viscoplastic deformation in amorphous solids", *Phys. Rev. E* **57** (1998), no. 6, p. 7192-7205.
- [131] M. Zink, K. Samwer, W. L. Johnson, S. G. Mayr, "Plastic deformation of metallic glasses: Size of shear transformation zones from molecular dynamics simulations", *Phys. Rev. B* **73** (2006), no. 17, article no. 172203.
- [132] Y. C. Hu, P. F. Guan, M. Z. Li, C. T. Liu, Y. Yang, H. Y. Bai, W. H. Wang, "Unveiling atomic-scale features of inherent heterogeneity in metallic glass by molecular dynamics simulations", *Phys. Rev. B* **93** (2016), article no. 214202.
- [133] K. E. Avila, S. Küchemann, I. A. Alhafez, H. M. Urbassek, "Shear-transformation zone activation during loading and unloading in nanoindentation of metallic glasses", *Materials* **12** (2019), no. 9, article no. 1477.
- [134] P. H. Mott, A. S. Argon, U. W. Suter, "Atomistic modelling of plastic deformation of glassy polymers", *Philos. Mag. A* **67** (1993), p. 931-978.
- [135] E. F. Oleinik, S. N. Rudnev, O. B. Salamatina, "Evolution in concepts concerning the mechanism of plasticity in solid polymers after the 1950s", *Polym. Sci. Ser. A* **49** (2007), p. 1302-1327.
- [136] A. S. Argon, H. Y. Kuo, "Plastic flow in a disordered bubble raft (an analog of a metallic glass)", *Mater. Sci. Eng.* **39** (1979), no. 1, p. 101-109.
- [137] D. Pan, A. Inoue, T. Sakurai, M. W. Chen, "Experimental characterization of shear transformation zones for plastic flow of bulk metallic glasses", *Proc. Natl. Acad. Sci.* **105** (2008), no. 39, p. 14769-14772.
- [138] G. Z. Voyiadjis, A. Samadi-Dooki, "Constitutive modeling of large inelastic deformation of amorphous polymers: Free volume and shear transformation zone dynamics", *J. Appl. Phys.* **119** (2016), article no. 225104.
- [139] E. R. Homer, C. A. Schuh, "Mesoscale modeling of amorphous metals by shear transformation zone dynamics", *Acta Mater.* **57** (2009), no. 9, p. 2823-2833.
- [140] E. R. Homer, D. Rodney, C. A. Schuh, "Kinetic Monte Carlo study of activated states and correlated shear-

- transformation-zone activity during the deformation of an amorphous metal”, *Phys. Rev. B* **81** (2010), no. 6, article no. 064204.
- [141] E. R. Homer, C. A. Schuh, “Three-dimensional shear transformation zone dynamics model for amorphous metals”, *Model. Simul. Mater. Sci. Eng.* **18** (2010), no. 6, article no. 065009.
 - [142] L. Li, E. R. Homer, C. A. Schuh, “Shear transformation zone dynamics model for metallic glasses incorporating free volume as a state variable”, *Acta Mater.* **61** (2013), no. 9, p. 3347-3359.
 - [143] V. V. Bulatov, A. S. Argon, “A stochastic model for continuum elasto-plastic behavior. I. Numerical approach and strain localization”, *Model. Simul. Mater. Sci. Eng.* **2** (1994), no. 2, p. 167-184.
 - [144] J. D. Eshelby, R. E. Peierls, “The determination of the elastic field of an ellipsoidal inclusion, and related problems”, *Proc. Math. Phys. Eng. Sci.* **241** (1957), no. 1226, p. 376-396.
 - [145] S. Im, Z. Chen, J. M. Johnson, P. Zhao, G. H. Yoo, E. S. Park, Y. Wang, D. A. Muller, J. Hwang, “Direct determination of structural heterogeneity in metallic glasses using four-dimensional scanning transmission electron microscopy”, *Ultramicroscopy* **195** (2018), p. 189-193.
 - [146] M. Mehdikhani, I. Straumit, L. Gorbatikh, S. V. Lomov, “Detailed characterization of voids in multidirectional carbon fiber/epoxy composite laminates using X-ray micro-computed tomography”, *Compos. Part A Appl. Sci. Manuf.* **125** (2019), article no. 105532.
 - [147] C. Breite, E. Schöberl, M. Mavrogordato, L. Gorbatikh, S. Lomov, Y. Swolfs, “Automated image analysis of ultrafast Synchrotron CT scans to experimentally characterise the fibre break development during in-situ tensile tests”, in *22nd International Conference on Composite Materials, Melbourne, Australia*, KU Leuven, 2019.
 - [148] X. Ni, R. Kopp, E. Kalfon-Cohen, C. Furtado, J. Lee, A. Arteiro, G. Borstnar *et al.*, “In situ synchrotron computed tomography study of nanoscale interlaminar reinforcement and thin-ply effects on damage progression in composite laminates”, *Compos. Part B Eng.* (2021), article no. 108623.
 - [149] E. Schöberl, C. Breite, S. Rosini, Y. Swolfs, M. Mavrogordato, I. Sinclair, S. Spearing, “A novel particle-filled carbon-fibre reinforced polymer model composite tailored for the application of digital volume correlation and computed tomography”, *J. Compos. Mater.* (2020), article no. 0021998320966388.